



Lagging behind: Impact of non-native gravel within a coastal dune system

Phillip P. Schmutz^{a,*}, Tynon Briggs^b, Samantha Seals^a

^a University of West Florida, Pensacola, FL, USA

^b Independent Researcher, Pensacola, FL, USA

ARTICLE INFO

Keywords:

Aeolian Transport

Coastal Dunes

Lag Surface

B-spline Regression

Non-erodible Roughness Elements

ABSTRACT

Recent research has increasingly focused on the intricate relationship between wind dynamics and sediment transport in coastal settings, particularly how surface features affect aeolian transport processes. Non-erodible roughness elements such as gravel or shell deposits play a significant role by altering wind flow and raising the wind velocity threshold required to mobilize sediment. Despite advancements in modeling, fully understanding sediment transport dynamics remains challenging due to the complex interactions between surface features and wind dynamics. This study explores the influence of non-erodible lag surfaces on sediment transport in sandy barrier island environments. Fieldwork on Santa Rosa Island, Florida, involved two plots: one with a natural sandy surface and another with a gravel lag surface. Wind and sediment transport were monitored for three months using cup anemometers and Wenglor particle counters. Spline regression models identified a two-knot system at wind speed thresholds of 9 ms^{-1} and 11 ms^{-1} , representing critical changes in sediment transport dynamics. Our results show that non-erodible surfaces significantly reduce sediment transport at lower wind speeds. At wind speeds below 9 ms^{-1} , sediment transport on the lag surface was 131 percent lower than on the non-lag surface. However, as wind speeds increased, the influence of the lag surface diminished, and no significant difference in transport was observed at wind speeds above 11 ms^{-1} . These findings emphasize the intricate role of non-erodible elements in reducing sediment transport at lower wind speeds while enhancing transport dynamics under stronger wind conditions. These insights inform future models and guide coastal management practices.

1. Introduction

In recent decades, research has increasingly focused on the complex interactions between wind dynamics and sediment transport in coastal environments, with particular attention to how various bed surface characteristics influence aeolian sediment transport (Walker et al., 2017). A wide range of studies have explored the impact of various factors, such as moisture content (e.g., Wiggs et al., 2004; Davidson-Arnott et al., 2008; Udo et al., 2008; Nield, 2011; Rotnicka, 2013; Swann et al., 2021), bed slopes (e.g., Iversen and Rasmussen, 2006; Barrineau and Ellis, 2013), vegetation (e.g., Arens, 1996; Lancaster and Baas, 1998; Gillies et al., 2006; Durán Vincent and Moore, 2013; Gillies and Lancaster, 2013), and armored non-erodible sediment surfaces (e.g., Gillette and Stockton, 1989; van der Wal, 1998; McKenna Neuman et al., 2012; Tan et al., 2013, 2016; Cheng et al., 2015) on aeolian transport dynamics. These investigations have highlighted the intricate relationships between micro-scale processes and meso-scale landform development in coastal dune systems.

Among the various bed surface characteristics, the presence of non-erodible roughness elements has emerged as a significant factor influencing aeolian sediment transport dynamics. Studies have shown that these non-erodible roughness elements introduce complexities to aeolian sediment transport dynamics, exerting a profound influence on the intricate interplay between wind dynamics and sediment transport processes by modulating the threshold shear velocity required for sediment mobilization (Sutton and McKenna Neuman, 2008; McKenna Neuman et al., 2013).

Despite decades of research and theoretical advancements, the predictive capabilities of existing models often fall short in accurately capturing observed aeolian sediment transport rates (Sherman and Li, 2012; Sherman et al., 2012). This gap between measured transport rates and model predictions underscores the complexity of sediment transport processes. A notable challenge is the tendency of theoretical models to overestimate transport rates, especially in scenarios where transport-limiting factors, such as non-erodible roughness elements, are not sufficiently considered. Owen's (1964) model, a cornerstone in aeolian

* Corresponding author.

E-mail addresses: pschmutz@uwf.edu (P.P. Schmutz), usvibriggs@gmail.com (T. Briggs), sseals@uwf.edu (S. Seals).

<https://doi.org/10.1016/j.aeolia.2024.100957>

Received 13 September 2024; Received in revised form 18 November 2024; Accepted 5 December 2024

Available online 19 December 2024

1875-9637/© 2024 Elsevier B.V. All rights are reserved, including those for text and data mining, AI training, and similar technologies.

geomorphology, provides a theoretical framework for predicting sediment fluxes over rough bed surfaces. However, more recent studies have stressed the need to account for transport-limiting influences, such as gravel patches and shell fragments, to improve predictions of sediment transport and dune formation. This study builds upon these insights by examining non-erodible lag surfaces in sandy barrier island environments, a context that has received less attention compared to arid desert regions.

1.2. Background

One of the earliest empirical studies exploring the effects of non-erodible roughness elements on sediment transport was conducted by Theodore Schlichting in 1936. Schlichting's pioneering experiments investigated the role of gravel and shell fragments in modifying wind-driven sediment transport processes. By systematically varying the size and distribution of spherical roughness elements on a bed surface, Schlichting (1936) demonstrated how non-erodible obstacles alter wind flow patterns and sediment transport rates. His observations laid the groundwork for subsequent research on the trapping and shielding effects of roughness elements in aeolian environments.

In the decades following Schlichting's pioneering work, researchers continued to explore the complex interactions between wind, sediment, and rough surfaces. A landmark contribution in this regard was the development of the "saltation-suspension" model by Owen (1964). Owen's model represented a significant advancement in understanding aeolian sediment transport, providing a theoretical framework for predicting sediment fluxes over rough bed surfaces. However, Owen's model oversimplified the role of non-erodible roughness elements, failing to capture the full complexity of their interactions with wind-driven sediment transport processes (Greeley and Iversen, 1985).

The advancement of computational modeling and instrumentation technologies in subsequent decades revolutionized the study of aeolian geomorphology, allowing researchers to study complex flow dynamics and sediment transport processes with unprecedented accuracy. This led to a resurgence of interest in the role of non-erodible roughness elements in shaping sediment transport dynamics. Collectively, these efforts have contributed to a deeper understanding of the mechanisms driving aeolian sediment transport and their implications for landscape evolution and environmental management.

1.3. Impact on sediment Transport

A variety of studies have shown that the presence of gravel surfaces profoundly influences sediment transport dynamics in aeolian environments, effectively altering wind flow patterns and sediment transport rates (e.g., Dong et al., 2004; Tan et al., 2013; Tan et al., 2016). Additionally, Nickling and McKenna Neuman (1995) and McKenna Neuman and Nickling (1995) provide insights into the development and behavior of deflation shell-lag surfaces on aeolian transport, which are relevant to understanding sediment transport patterns in coastal dune environments.

Gravel and shell-covered beds exemplify the pronounced effects of non-erodible elements on sediment transport in coastal systems. A key mechanism by which these elements exert their influence is by redistributing wind shear stress across the bed surface. Raupach et al. (1993) and McKenna Neuman and Nickling (1995) elucidated this phenomenon by demonstrating that non-erodible roughness elements absorb a portion of the wind energy, effectively partitioning the wind shear stress along the bed. As a result, the shear velocity threshold required to initiate sediment transport increases, hindering the mobilization of sediment particles. Sutton and McKenna Neuman (2008) and Tan et al. (2013) highlight the trapping effect of roughness elements, which impedes the movement of sand particles. These studies reveal that such roughness elements not only increase the threshold friction velocity but also alter the spatial distribution of wind-induced stresses, leading to

microscale variations in sediment transport rates.

The impact of non-erodible roughness elements on sediment transport extends beyond modifying wind energy distribution and shear velocity thresholds. Their presence elevates the bed surface roughness, intensifying the trapping effect on sediment particles. Hoonhout and de Vries (2016) observed that the increased roughness height leads to enhanced turbulent flow structures near the bed surface, further impeding sediment transport. Consequently, the presence of non-erodible elements not only raises the threshold for sediment transport initiation but also creates additional barriers to sediment movement, altering sediment transport patterns and redistributing sediment across the landscape.

Despite progress in understanding the effects of non-erodible roughness elements on sediment transport, several challenges persist. These studies collectively highlight the need to integrate theoretical models with empirical field research to develop a more comprehensive understanding of aeolian sediment transport dynamics and their implications for coastal geomorphology. The intricate interactions between sediment characteristics, bed surface roughness, and wind dynamics require further investigation. Combining theoretical models with empirical data is crucial for building robust predictive frameworks that can more accurately forecast sediment transport dynamics in aeolian environments. Addressing these challenges will not only deepen our understanding of core geomorphic processes but also inform effective strategies for coastal management and environmental conservation.

1.4. Models, lab Experiments, and field studies

Existing models inadequately delineate the distinction between transport capacity and sediment availability in relation to bed surface properties. While Owen's (1964) model provides a foundational framework, contemporary research underscores the need for more refined models that account for the intricate interrelationships between sediment characteristics, bed surface roughness, and wind dynamics (Bennett et al., 2015). Bridging the gap between theoretical models and empirical observations is crucial for enhancing our understanding of aeolian sediment transport dynamics in real-world settings.

Lab experiments allow for controlled manipulation of bed surface properties and environmental variables, enabling researchers to isolate the effects of non-erodible roughness elements on sediment transport (McKenna Neuman, 1998; McKenna Neuman et al., 2012; McKenna Neuman et al., 2013; McKenna Neuman and Bédard, 2017). These experiments provide valuable insights into the mechanisms of sediment transport under specific conditions that may be challenging to replicate in the field. The findings from lab studies often serve as a foundation for developing theoretical models that aim to capture the complex dynamics of aeolian sediment transport. While lab experiments provide controlled conditions, theoretical models extend these findings by creating generalized frameworks that can predict sediment transport across various natural settings. By validating model outputs against field data, researchers can assess the robustness of these models and identify areas where model predictions diverge from real-world observations, indicating potential avenues for further refinement (Dong et al., 2012; Tan et al., 2013; Tan et al., 2016). This process of aligning lab, theoretical, and field studies strengthens our understanding of aeolian sediment transport and improves the models' applicability to natural environments.

While significant progress has been made in understanding the impact of non-erodible roughness elements on sediment transport, challenges remain in effectively integrating theoretical models with empirical field studies (Walker et al., 2017). Field studies, particularly those involving long-term monitoring of lag surfaces, are crucial for capturing the complexities of sediment dynamics under diverse and variable environmental conditions. Through these monitoring programs, researchers can gather comprehensive data on sediment transport rates, grain size distributions, and wind velocities over time, all of

which are essential for validating and refining theoretical models. This iterative validation process not only improves the robustness of theoretical frameworks but also highlights areas where models may fall short when applied to natural, uncontrolled environments.

Furthermore, these field-based insights have practical applications beyond theoretical advancement. The data obtained from long-term monitoring and model validation can directly inform coastal management and environmental conservation strategies. By improving our predictive understanding of sediment transport in natural settings, researchers can help coastal managers anticipate erosion patterns, evaluate the resilience of coastal dunes, and develop more effective approaches to preserving fragile ecosystems. In this way, the integration of lab, theoretical, and field studies not only advances the scientific understanding of aeolian processes but also provides tangible benefits for managing and conserving coastal landscapes.

2. Methods

2.1. Study area

The field site for this study was located on an undeveloped portion of Santa Rosa Island, Florida, approximately two miles east of Pensacola Beach (Latitude: 30.350°, Longitude: -87.044°). The island features a discontinuous foredune system, with dunes reaching up to 7 m in height and an average elevation of 3 to 4 m above mean sea level (2 to 3 m above beach grade) (Claudino-Sales et al., 2010). The interior and back-barrier areas are characterized by dune hummocks, sand flats, shrub forests, and wetland grasses. The sediment is primarily quartz (99 percent) with a mean grain size of 0.33 mm (Houser and Barrett, 2009). The sediment originates from an eroding pre-Holocene headland in the central Florida panhandle (Stone et al., 1992; Stone and Stapor, 1996) and reworked sediments deposited on the inner continental shelf during lower sea levels during the Pleistocene (Rucker and Snowden, 1989). Additionally, there are extensive gravel and asphalt substrates scattered throughout the sand flats, remnants of the destruction of County Road 399 during hurricanes Ivan (2004) and Dennis (2005), contributing to a substantial lag surface over the years (Houser et al., 2008; Houser, 2009).

The region has a mild, subtropical climate, with an average annual precipitation of 150 cm. Frequent storm systems occur from October through June, primarily originating from advancing fronts from the northwest, while tropical systems impact the area in the summer and early fall (Miller et al., 2001). These events often produce periods of high winds, waves, and storm surges, resulting in shoreline erosion, dune retreat, and overwash. Wind direction is tri-modal, with prevailing winds from the southeast, and high-velocity winds often coming from the southwest and northwest during frontal storm events (Schmutz et al., 2019).

2.2. Field Methods

The research site was situated in a topographically flat area covering 1.25 ha in the central portion of Santa Rosa Island. To minimize wind flow disturbance from the surrounding dunes and maximize transport fetch, careful consideration was given to site selection. The nearest dunes to the instrument array were approximately 35 m away, with most located at distances greater than 40 m. The study site consisted of two 10 m x 10 m plots: one cleared of all non-native gravel to reflect the natural quartz sand surface of the island, and the other left undisturbed, retaining the gravel lag concentration. The plots were positioned slightly offset to north, approximately 15 degrees in northeast/southwest orientation, about 10 m apart, with the clear non-lag plot positioned to the north.

Data collection occurred continuously from March 3 to May 31, 2017. Wind data gathered from a National Centers for Environmental Information (NCEI) weather station, located 18 km away in Pensacola

Bay, revealed that this period had the highest concentration of wind events exceeding the estimated sediment transport velocity threshold for Santa Rosa Island. Wind speed and direction were measured using cup anemometers positioned at 0.25, 0.5, 1.0, and 2.0 m and wind vane at 2.5 m. While measurements at multiple heights provide a comprehensive view of wind shear profiles, for this study, we focused our analysis on wind data from a single height at 2 m. By standardizing to a single height, we reduce the dataset's dimensionality, which simplifies the analysis due to the longer temporal aspect of the study, thus enhancing the model's statistical power. This approach minimizes variability introduced by different frictional layers near the surface, resulting in a more consistent dataset that enables clearer statistical relationships between wind fluctuations and sediment transport. Focusing on one height also reduces the potential for multicollinearity, which can arise when measurements at different heights are highly correlated, thereby improving the reliability of the regression model. Shear velocity was estimated for each surface by identifying threshold wind speeds associated with the onset of sediment transport, derived from transport count data, and applying the law-of-the-wall equation. For the cleared surface, a standard roughness length was used, while for the lag surface, the roughness value was adjusted to reflect its non-erodible characteristics and refined to match observed transport activity.

Sediment transport was monitored using Wenglor particle counters placed approximately 3.0 cm above the bed surface at the center of each plot. The sensors were mounted on 360-degree omni-directional rotating devices, enabling them to automatically adjust to shifts in wind direction (Schmutz et al., 2019). The surface of the cleared plot was inspected weekly to remove any remnant lag uncovered due to transport activity. All instruments were connected to a Campbell Scientific CR1000 data-logger, which recorded data at 1 Hz, logging wind speed, direction, and sediment transport activity (via Wenglor counts) every minute.

2.3. Data analysis

The overall goal of the statistical model was to quantify sediment transport as a function of wind speed between the two field plots. Because transport was calculated as count data via the Wenglor sensors, it was modeled using negative binomial regression, a generalized linear model. General linear models, which include ordinary least squares regression do not allow for modeling of non-continuous outcomes. Under ordinary least squares, the model is:

$$y = \beta_0 + \beta_1 x_1 + \dots + \beta_k x_k + \varepsilon$$

where y is the continuous outcome of interest, β_0 is the y -intercept, β_i is the slope corresponding to x_i , and ε is the random error term (Agresti, 2015).

However, generalized linear models extend the general linear model and allow for the modeling of non-continuous outcomes; Poisson and negative binomial regressions are appropriate for count outcomes. While Poisson regression assumes the mean and variance of the outcome to be the same, negative binomial is more flexible and does not. Because the variance of sand transport was much larger than the mean ($\text{lag} \bar{x} = 640$ and $s^2 = 5105449$, no lag: $\bar{x} = 1286$ and $s^2 = 6000292$), negative binomial regression was chosen. Under negative binomial regression, the model is:

$$\ln(y) = \beta_0 + \beta_1 x_1 + \dots + \beta_k x_k$$

where y is the continuous outcome of interest, β_0 is the y -intercept, β_i is the slope corresponding to x_i (Agresti, 2015).

It is important to note the difference in the modeled outcomes; specifically, under negative binomial regression, $\ln(y)$ is modeled rather than y directly. As such, transformation of the estimated relationships, $\hat{\beta}_i$, is necessary to understand the impact on y directly. By exponentiating the slope, interpretation as related to y can be made. This expo-

mentation, e^{β_i} , is called the incidence rate ratio (IRR) and now is a multiplicative effect, rather than an additive effect as in ordinary least squares regression. An IRR > 1 indicates an increase in the count, an IRR < 1 indicates a decrease in the count, and IRR = 1 indicates no change in the count (Agresti, 2015). Interpretations may be stated as percent increases or decreases. For example, an IRR of 1.5 indicates a 50 percent increase as the count is being multiplied by 1.5 $((1.5-1)100\% = 50\%)$, and an IRR of 0.6 indicates a 40 percent decrease as the count is being multiplied by 0.6 $((1-0.6)100\% = 40\%)$ as wind speed increases. In this context, the IRR can be viewed as a measure of the system's sensitivity to transport counts in response to wind fluctuations.

In regression analysis, slopes are typically assumed to be constant. However, knots, or breakpoints, can be constructed to model different slopes in transport activity under varying wind speeds (Harrell, 2015). For example, inclusion of a single knot would allow for two slopes: the slope from the minimum to the breakpoint and the slope from the breakpoint to the maximum. In the current analysis, spline regression models were constructed to quantify differences in aeolian transport activity via Wenglor counts between the lag and no lag bed surfaces.

To establish the knot locations for wind speed, the wind regime was stratified into 0.5 ms^{-1} wind speed units and candidate models were examined for optimal knot placement. Optimal knot placement was determined using the Bayesian Information Criterion (BIC). The BIC is defined as:

$$BIC = -2\ln(L) + k\ln(n),$$

where n is the sample size, and L is the maximum value of the likelihood function for the estimated model, and k is the number of predictors included in the model. Among the models under consideration, the model with the lowest BIC score is preferred; however, the terms “large” or “small” BIC values carry no inherent meaning (Schwarz, 1979). This approach produced a dual knot model signifying three distinct segments of transport activity across the measured wind speeds with three unique slopes to describe the relationship between sand transport and wind speed: minimum wind speed to the first wind speed knot, first knot to the second wind speed knot, and the second knot to the maximum wind speed. This implies that the relationship between sand transport and wind speed is no longer constant for any wind speed but varies depending on wind speed.

To determine statistical differences in transport activity between plots with and without lag, interaction terms were included for each segment of the model. When the coefficients of the interaction terms are significantly different from zero, the slope of sand transport in the lag

plot and the slope of sand transport for the plot without lag may be assumed different, thus providing justification for stratifying the models. That is, one model for a sediment surface with lag and, separately, another model for the sediment surface without lag were constructed.

Statistical analysis was performed using Stata Version 16.1 (StataCorp, 2020) and graphs were created using R in R Studio (R Core Team, 2024). Statistical significance was defined *a priori* as $p < 0.05$.

3. Results

3.1. Wind field

Wind speed recorded at two-meter elevation over the three-month study period ranged from 0 to 17.8 ms^{-1} (Fig. 1). The predominant wind direction was from the southeast; however, the overall wind field displayed a tri-modal pattern, with substantial contributions from the northwest and southwest. These three directional patterns accounted for 72 percent of all winds and 79 percent of winds exceeding the estimated threshold friction velocity (u_{*c}) of 0.26 ms^{-1} (equivalent to a wind speed of 5.9 ms^{-1} at elevation of two meters), as calculated using the Bagnold model (1941).

Fig. 1 also presents sand roses, correlating wind direction with transport activity measured by the single rotating Wenglor device in the lag and non-lag plots. In both plots, sediment transport followed a tri-modal distribution pattern with slight variations in the dominant direction. In the lag plot, transport activity was observed over a wind speed range of 6.5 to 15.1 ms^{-1} at two meters (u_{*c} of $0.29 - 0.67\text{ ms}^{-1}$). In contrast, the non-lag plot recorded transport at wind speeds ranging from 5.0 and 15.1 ms^{-1} at two meters (u_{*c} of $0.22 - 0.67\text{ ms}^{-1}$).

3.2. Lag vs Non-Lag transport activity

3.2.1. Lag vs Non-Lag statistical model

To explore the optimal knot placement, dual spline knot models were constructed with varying knots. The BIC for each model was evaluated, with the lowest value indicating the best-fitting model among the candidates (see Section 2.3 for a detailed explanation of the BIC). The best-fit model identified by the BIC established knots at wind speeds of 9 ms^{-1} and 11 ms^{-1} (Fig. 2). This model revealed significantly different relationships with sediment transport activity between the lag and non-lag plots for wind speeds less than 9 ms^{-1} ($p < 0.001$) and wind speeds between 9 ms^{-1} and 11 ms^{-1} ($p = 0.001$). However, for wind speeds greater than 11 ms^{-1} , no significant difference was observed between

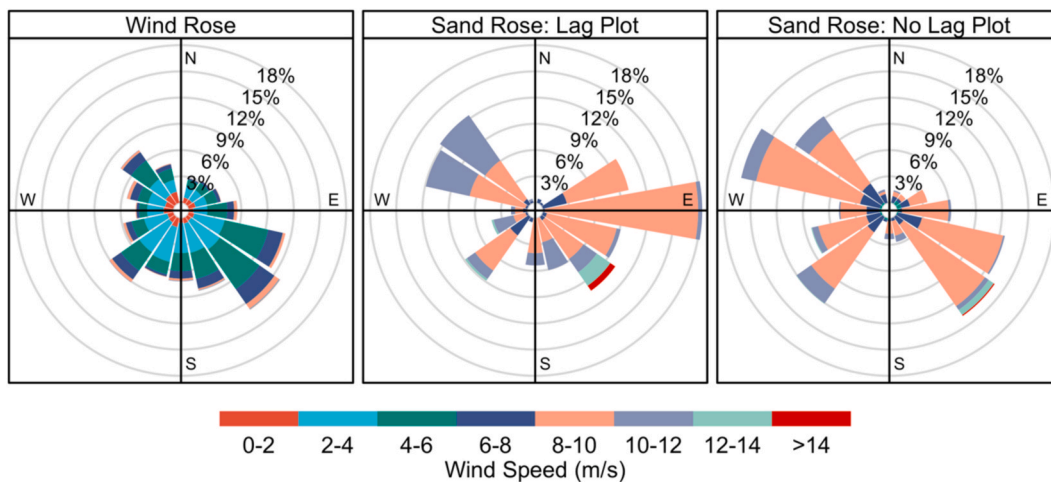


Fig. 1. Wind rose (left) depicting the frequency distribution of wind speed and direction measured at a 2.0 m elevation during the entire three-month study period. Sand roses (middle and right) illustrate the frequency of winds (speed and direction) that initiated sediment transport, as measured by the Rotating Wenglor Device (RWD) in the Lag and No Lag plots. Wind and sand rose diagrams were generated using the Openair package in R (Carslaw and Ropkins, 2012).

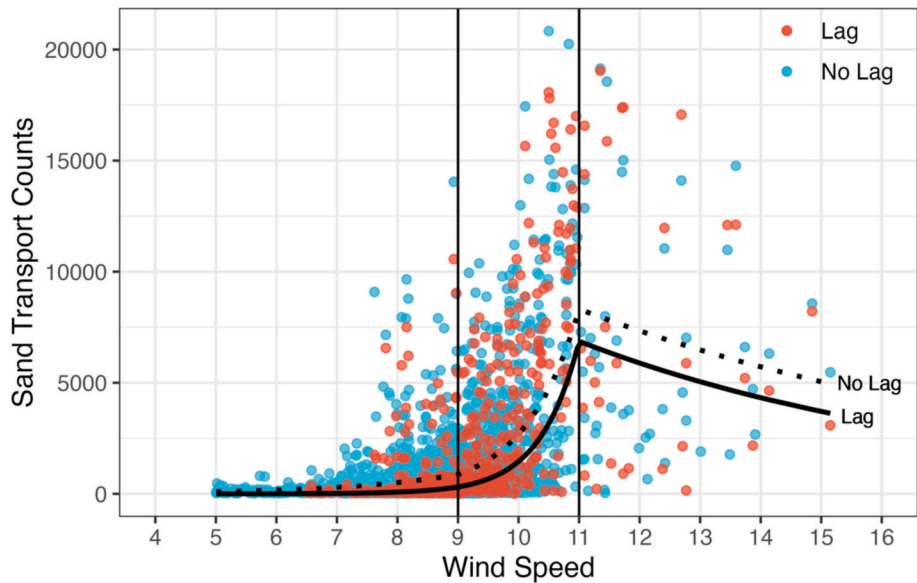


Fig. 2. Scatter plot depicting sand transport counts as a function of wind speed for the Lag (red) and No Lag (blue) plots. The solid black line represents the regression model for the Lag conditions, while the dotted line illustrates the regression model for the No Lag conditions. Vertical lines indicate wind speed thresholds (knots) identified by the Bayesian Information Criterion (BIC) model. (For interpretation of the references to colour in this figure legend, the reader is referred to the web version of this article.)

the two plots ($p = 0.841$).

These findings indicate the presence of multiple unique transport mechanisms within the system. First, there is a distinction between higher and lower wind speeds, as evidenced by the spline knot at 11 ms^{-1} . This knot signifies a statistical difference in transport activity above and below this wind speed. At wind speeds greater than 11 ms^{-1} , the two plots function statistically the same, whereas for wind speeds below 11 ms^{-1} , transport activity in the two plots is statistically different. The second distinction is marked by the presence of a spline knot at 9 ms^{-1} within the lower wind speed range. This knot illustrates that transport activity at these lower wind speeds is not the same between the two plots, although both plots were statistically different from each other.

Because of the significant differences in the relationships between lag and non-lag plots, we stratified the model to explore the differences between the plot surfaces (Table 1). For the low ($< 9\text{ ms}^{-1}$) and medium ($9\text{--}11\text{ ms}^{-1}$) wind speed ranges, we see that as wind speed increases, the amount of sand being transported also increases (all $p < 0.001$), as expressed by an incidence rate ratio (IRR) value greater than 1. However, the two plots behave differently with respect to their sensitivity to changes in wind speed. Example interpreting of the IRR for the no lag plot at low wind speeds: for a 1-unit change in wind speed, the amount of sand transported is multiplied by a factor of 1.72 ($p < 0.001$), indicating

a 72 percent change in transport activity. In contrast, for the lag plot, a 1-unit change in wind speed is associated with 4.04-fold adjustment ($p < 0.001$), representing a 304 percent change in transport activity. Although not statistically significant, for high wind speeds, as wind speed increases, the amount of sand being transported decreases (all $p > 0.3$). The IRR values are below 1 indicating a reduction in transport activity for a 1-unit change in wind speed. We acknowledge that secondary controls, such as precipitation and the limited number of observations (92 over the 3-month study period), may influence the reduction in transport activity at this higher wind speed regime. Further investigation of this relationship is warranted as additional data become available.

3.2.2. Transport mass

A notable limitation of the Wenglor sensor is that it outputs particle count rates, which do not directly correspond to aeolian transport flux or mass balance assessments. While particle count data are frequently reported in the aeolian literature, this approach limits the ability to make cross-study comparisons (Barchyn et al., 2011). To address this limitation, we applied the model developed by Barchyn et al. (2014) to estimate mass flux from Wenglor particle counts for each plot.

The results indicate that the total mass of transport in the non-lag plot was more than twice that of the lag plot over the three-month study period—2.6 million particle counts calculated to 940 kg of transport mass, compared to 1.23 million particle counts and 458 kg of transport mass, respectively (Table 2). During periods of lower wind speeds, below the 9 ms^{-1} knot value, the total mass transported within the non-lag plot was nearly five times greater than that of the lag

Table 1
Regression estimates, incidence rate ratios (IRRs), and p-values for the Lag and No Lag plots, stratified by the three wind speed groups.

| Wind Speeds | Lag Plot | | | No Lag Plot | | |
|-------------------------------|---------------------|-------------------|-----------|---------------------|-------------------|-----------|
| | Estimate (95 % CI) | IRR (95 % CI) | p-value | Estimate (95 % CI) | IRR (95 % CI) | p-value |
| $< 9\text{ ms}^{-1}$ | 1.40 (0.90, 1.85) | 4.04 (2.45, 6.39) | < 0.001 | 0.54 (0.47, 0.61) | 1.72 (1.60, 1.84) | < 0.001 |
| $9\text{--}11\text{ ms}^{-1}$ | 1.55 (0.96, 2.22) | 4.71 (2.62, 9.19) | < 0.001 | 1.13 (1.01, 1.25) | 3.09 (2.74, 3.50) | < 0.001 |
| $> 11\text{ ms}^{-1}$ | -0.15 (-0.96, 1.71) | 0.86 (0.64, 1.08) | 0.799 | -0.13 (-0.33, 0.12) | 0.88 (0.72, 1.13) | 0.303 |

Table 2
Total mass (kg) of transported material in the Lag and No Lag plots. Transport mass also distributed by wind speed knot range.

| Wind Speeds | Mass Flux (kg) | | % of Total Mass | | % of Total Wind Field | |
|-------------------------------|----------------|-----|-----------------|--------|-----------------------|-------------------|
| | No Lag | Lag | No Lag | Lag | All Winds | Transporting Wind |
| $< 9\text{ ms}^{-1}$ | 249 | 52 | 26.4 % | 11.3 % | 98.5 % | 59.6 % |
| $9\text{--}11\text{ ms}^{-1}$ | 591 | 315 | 62.8 % | 68.9 % | 1.3 % | 39.4 % |
| $> 11\text{ ms}^{-1}$ | 101 | 91 | 10.7 % | 19.9 % | 0.2 % | 0.97 % |

plot—249 kg versus 52 kg, respectively. As wind speeds increased from 9 ms^{-1} to the 11 ms^{-1} knot value, approximately twice as much sediment was transported in the non-lag plot compared to the lag plot. However, as wind speeds exceeded the 11 ms^{-1} knot value, the discrepancy in mass flux between the two plots diminished, with 100 kg transported in the non-lag plot versus 94 kg in the lag plot.

Overall, these data support the findings from our statistical model, which identified significant differences in transport activity within the two research plots at lower wind speed regimes, but no significant difference for the highest wind speed regime.

4. Discussion

4.1. Aeolian transport dynamics

Our data align with prior research, confirming that non-erodible surface elements significantly influence aeolian processes by increasing surface roughness, thereby raising the threshold wind velocity required for sediment entrainment (Gillette & Stockton, 1989; Raupach et al., 1993). The threshold friction velocity (u_{*c}) for the lag surface was 0.29 ms^{-1} , compared to 0.22 ms^{-1} for the non-lag surface, indicating that the non-erodible elements increased the required threshold by 1.3 times.

This difference is further illustrated by the pronounced disparity in incident rate ratios (IRR) values between the two plots, highlighting the lag surface's heightened sensitivity to changes in wind velocity. The larger IRR for the lag surface plot indicates that the system is more sensitive to fluctuations in wind shear, even a slight decrease in wind velocity results in a notable reduction in sediment transport. Specifically, the model estimates a 304 percent change in transport activity for wind speeds below 9 m/s on the lag surface ($\text{IRR}_{\text{lag}} = 4.04$). In contrast, the non-lag surface demonstrates markedly less sensitivity, with only a 72 percent change in transport activity ($\text{IRR}_{\text{non-lag}} = 1.72$). This difference is further corroborated by mass transport estimates within this lower wind regime, where only 52 kg of sediment was transported on the lag surface compared to 249 kg on the non-lag surface. These results align with existing literature, which suggests that non-erodible elements on the lag surface absorb a portion of the wind energy, thereby inhibiting the mobilization of sediment particles.

However, as wind speeds increase, the influence of non-erodible elements on transport diminishes, a trend supported in the literature by McKenna Neuman and Nickling (1995), Mikami et al. (2005), Tan et al. (2013, 2016), Valance et al. (2015), and Delorme et al. (2023). In our study, no significant differences in transport were observed between the two surfaces at wind speeds greater than 11 ms^{-1} ($\text{IRR}_{\text{lag}} = 0.86$, $\text{IRR}_{\text{non-lag}} = 0.88$). However, the percentage of transported mass was nearly doubled for the lag surface compared to the non-lag surface. This pattern was also evident in the middle wind speed regime ($9\text{--}11 \text{ ms}^{-1}$), where the lag surface experienced nearly half the mass transport of the non-lag surface, but the percentage of transported mass remained higher on the lag surface ($\text{IRR}_{\text{lag}} = 4.71$, $\text{IRR}_{\text{non-lag}} = 3.09$). These findings align with the work of Tan et al. (2013, 2016). The authors determined that higher wind speeds lead to more dynamic grain-bed interactions. Saltation collisions become more elastic at higher velocities, increasing saltation height, rebound angle, and impact velocity, thereby enhancing the transport capacity of the lag surface. Thus, while lag surfaces reduce sediment transport at lower wind speeds, they may contribute to enhanced transport dynamics at higher wind speeds, depending on the wind intensity and the spatial distribution of non-erodible elements. These findings highlight the dual nature of lag surfaces: they mitigate sediment transport under low wind speeds but have the potential to amplify transport processes under stronger wind conditions, driven by the dynamics of grain-bed interactions and wind shear fluctuations.

4.2. Spline regression models

The application of spline modeling offers a robust statistical framework for analyzing data related to sediment transport dynamics, particularly in aeolian environments where multiple interacting variables contribute to the complexity of the system. Unlike traditional linear models, spline analysis captures non-linear relationships and abrupt changes in sediment transport that often occur in aeolian systems. This method would be particularly beneficial in environments where aeolian processes are influenced by multiple variables, such as wind speed, surface roughness, moisture content, and the presence of non-erodible elements (Hoonhout and De Vries, 2016).

For example, spline models can be used to pinpoint the thresholds at which sediment transport is initiated or halted under varying environmental conditions. By adjusting the number and placement of knots, researchers can better model the underlying physical processes that govern aeolian transport, revealing subtle but important changes in the relationship between wind shear and sediment entrainment.

One of the key advantages of spline modeling is its ability to model threshold-dependent behaviors, which are common in aeolian systems and often obscured by more simplistic linear approaches (Baas, 2007). A spline model could account for these threshold behaviors, offering a more detailed understanding of how sediment transport changes under different environmental conditions. The model allows for the placement of knots at critical breakpoints where there is a significant change in the rate of sediment transport. By adjusting the number and placement of knots, researchers can better model the underlying physical processes that govern aeolian transport, revealing subtle but important changes in the relationship between wind shear and sediment entrainment. This is particularly important in aeolian transport, where localized interactions between wind flow and surface conditions create a highly variable environment. As our study illustrated, the presence of non-erodible objects can both enhance and suppress sediment transport. In some cases, wind flowing over or around non-erodible features creates more dynamic grain-bed interactions, enhancing sediment entrainment, while in other cases, these objects create sheltered zones that reduce wind energy and therefore limit sediment transport (Tan et al., 2013, 2016; de Moraes et al., 2019). Spline analysis enables researchers to model these localized effects in ways that traditional linear models cannot.

Furthermore, aeolian systems are often characterized by spatial heterogeneity, with patches of varying roughness, sediment availability, and moisture content. These patches can lead to highly localized differences in sediment transport, as wind interacts with surfaces in uneven ways. By allowing for different knots, or threshold points in the analysis, spline models can adapt to these spatial variations, providing a much more granular view of transport dynamics than simpler models.

Despite its clear advantages, spline modeling remains an underutilized tool in the aeolian literature. This statistical method could provide new insights into the complexity of sediment transport dynamics, particularly in heterogeneous aeolian environments. By offering a flexible and precise way to model the non-linearities inherent in aeolian processes, spline modeling could enhance our understanding of how environmental factors like turbulence, surface roughness, and sediment availability affect sediment transport. Incorporating this method into more aeolian studies could lead to improved predictive models and better land management strategies.

4.3. Control on Morphological development

These findings have significant implications for understanding long-term dune development. Research by Durán Vincent and Moore (2015) and Houser et al. (2015) emphasizes that the resilience of barrier islands is closely tied to the ability of their beach and dune systems to recover following intense storm events. These studies highlight the marked temporal differences in recovery rates, with beach systems typically

recovering within weeks to months, whereas dune systems may take years or even decades.

Our statistical analysis, which examines transport activity under and above the 11 ms^{-1} wind speed threshold, demonstrates that the cleared, non-lag surface notably enhances sediment transport compared to the lag-covered surface during these conditions. Notably, wind speeds exceeding the 11 ms^{-1} threshold occurred in less than two percent of all recorded wind events over the three-month observation period. This underscores that the presence of gravel lag substantially diminishes aeolian transport activity for over ninety-eight percent of the time, highlighting the differential impacts of lag material on sediment transport across varying wind speed regimes. This, in turn, depicts the extended time required for dune development and recovery following storm events.

In this context, our research positions Santa Rosa Island as a vulnerable barrier system in which the substantial presence of lag material across the dune landscape significantly hinders the system's resilience by impeding sediment transport and thus dune growth. This study contributes to the broader understanding of barrier island dynamics by demonstrating how the anthropogenic gravel lag inhibits recovery, thereby extending the time required for dune development and recovery on the island following storm events.

4.4. Management Implication

The question arises: should the non-native gravel substrate be removed from the natural sand system, or should it remain? This is a pertinent question due to the significant monetary costs associated with removal. In 2016, the National Park Service (NPS) initiated a five-year \$10.85 million project, funded through the Deepwater Horizon Natural Resource Damage Assessment (NRDA), to remove weathered asphalt chunks from approximately 500 ha within Gulf Islands National Seashore (Gabriel, 2016, 2017). The primary objective of the NPS project was to improve the visual appeal for park visitors; however, our data indicate the long-term positive impact these efforts will have on the dune system.

Escambia County and the Pensacola Beach community have been hesitant to the removal of this material, questioning the long-term feasibility of the clean-up. Local citizens and community leaders are concerned about the need for repeated clean-up efforts after each storm and the potential negative environmental impact that heavy machinery may have on coastal biota and nesting shorebirds (Gabriel, 2018). Christian Wagley, a spokesman for the Gulf Restoration Network, stated that while the asphalt removal project offers some short-term benefits, the presence of the road will necessitate ongoing clean-up efforts as it continues to wash out.

Monetarily, we concur with their concerns. However, this study highlights the environmental benefits of the NPS clean-up efforts in enhancing aeolian transport and promoting long-term dune development. By investing in the removal of lag material, dune growth could accelerate, potentially mitigating the impact of future storms and preventing overwash events that would damage the road system and generate the problematic asphalt and gravel lag material. Additionally, environmental management initiatives often focus on the preservation and conservation of biological specimens, with little emphasis on abiotic coastal dune landscapes. Studies have shown that dune environments provide significant ecological and economic services (Silva et al. 2016; Sigren et al. 2018). Jackson et al. (2020) found that despite increased sea level rise, enhanced protection of coastal dune habitats could reduce potential residential property damage from tropical storm systems by tens of millions of dollars. Thus, coastal management funding should also consider restoration initiatives such as the removal of gravel lag to promote natural dune evolution.

5. Conclusion

This research experiment provided empirical data on sediment transport activity within varying bed surface layers in a coastal environment. Sediment transport was compared across two surfaces: one with the natural sand composition of the coastal system and another with the natural sands mixed with a moderate concentration of anthropogenically introduced gravel. The experiment aimed to evaluate the impact of this intrusive, anthropogenic gravel lag on aeolian sediment transport activity and to determine if removing the gravel lag would facilitate increased transport.

Results from our project confirm that the presence of gravel in the bed surface layer significantly controls sediment transport activity. Our data indicate that the gravel lag significantly reduces aeolian transport at lower wind speeds; however, as wind speed increases, the dynamics of sediment transport become more complex, and no significant differences in transport activity were observed between the two sediment surfaces. The wind speed threshold at which the presence of gravel lag ceased to significantly influence sediment transport activity was found to be 11 ms^{-1} . Notably, ninety-eight percent of all recorded wind speeds were below this threshold.

Overall, our findings demonstrate the significant impact of gravel lag on transport activity and its potential adverse effects on dune development in the region. Removal of the lag material could be crucial for promoting dune growth on Santa Rosa Island, Florida. These results can help inform coastal engineering and management practices in regions with naturally varying or anthropogenically induced bed surface characteristics.

CRediT authorship contribution statement

Phillip P. Schmutz: Writing – review & editing, Writing – original draft, Visualization, Resources, Project administration, Methodology, Investigation, Formal analysis, Data curation, Conceptualization. **Tynon Briggs:** Writing – original draft, Methodology, Investigation, Conceptualization. **Samantha Seals:** Writing – review & editing, Visualization, Formal analysis, Data curation.

Declaration of competing interest

The authors declare that they have no known competing financial interests or personal relationships that could have appeared to influence the work reported in this paper.

Acknowledgements

The authors thank the two anonymous reviewers for their valuable feedback and constructive suggestions, which greatly improved this manuscript. We also extend our gratitude to Dr. Amy Potter for inspiring the title of this study. This research was supported in part by a UWF Office of Undergraduate Research Grant awarded to T.B. and a Faculty Research Grant from the UWF Office of Research Administration and Engagement awarded to P.P.S.

Data availability

Data will be made available on request.

References

- Agresti, A., 2015. *Foundations of Linear and Generalized Linear Models*. Wiley.
- Arens, S.M., 1996. Patterns of sand transport on vegetated foredunes. *Geomorphology* 17, 339–350. [https://doi.org/10.1016/0169-555X\(96\)00016-5](https://doi.org/10.1016/0169-555X(96)00016-5).
- Baas, A.C.W., 2007. Complex systems in aeolian geomorphology. *Geomorphology* 91 (3–4), 311–331. <https://doi.org/10.1016/j.geomorph.2007.04.012>.
- Bagnold, R.A., 1941. *The physics of blown sand and desert dunes*. Methuen & Co., Ltd, London.

- Barchyn, T.E., Hugenholtz, C.H., 2011. Comparison of four methods to calculate aeolian sediment transport threshold from field data: Implications for transport prediction and discussion of method evolution. *Geomorphology* 129, 190–203. <https://doi.org/10.1016/j.geomorph.2011.01.022>.
- Barchyn, T.E., Hugenholtz, C.H., Li, B., Neuman, C.M., Sanderson, R.S., 2014. From particle counts to flux: Wind tunnel testing and calibration of the ‘Wenglor’ aeolian sediment transport sensor. *Aeolian Res.* 15, 311–318. <https://doi.org/10.1016/j.aeolia.2014.06.009>.
- Barrineau, C., Ellis, J., 2013. Sediment transport and wind flow around hummocks. *Aeolian Res.* 8, 19–27. <https://doi.org/10.1016/j.aeolia.2012.10.002>.
- Bennett, S.J., Ashmore, P., McKenna Neuman, C., 2015. Transformative geomorphic research using laboratory experimentation. *Geomorphology* 244, 1–8. <https://doi.org/10.1016/j.geomorph.2014.11.002>.
- Carslaw, D.C., Ropkins, K., 2012. Openair — an R package for air quality data analysis. *Environ. Model. Softw.* 27, 52–61. <https://doi.org/10.1016/j.envsoft.2011.09.008>.
- Cheng, H., Liu, C., Zou, X., Li, J., He, J., Liu, B., Wu, Y., Kang, L., Fang, Y., 2015. Aeolian creeping mass of different grain sizes over sand beds of varying length. *J. Geophys. Res.* Earth Surf. 120, 1404–1417. <https://doi.org/10.1002/2014JF003367>.
- Claudino-Sales, V., Wang, P., Horwitz, M.H., 2010. Effect of Hurricane Ivan on coastal dunes of Santa Rosa Barrier Island, Florida: characterized on the basis of pre- and poststorm LIDAR surveys. *J. Coast. Res.* 26 (3), 470–484.
- Davidson-Arnott, R.G.D., Yang, Y., Ollerhead, J., Hesp, P.A., Walker, I.J., 2008. The effects of surface moisture on aeolian sediment transport threshold and mass flux on a beach. *Earth Surf. Proc. Land.* 33, 55–74. <https://doi.org/10.1002/esp.1527>.
- de Morais, C.L., Ferreira, M.C.S., Santos, J.M., Furieri, B., Harion, J.-L., 2019. Influence of non-erodible particles with multimodal size distribution on aeolian erosion of storage piles of granular materials. *Environ. Fluid Mech.* 19 (3), 583–599. <https://doi.org/10.1007/s10652-018-9640-6>.
- Delorme, P., Nield, J.M., Wiggs, G.F.S., Baddock, M.C., Bristow, N.R., Best, J.L., Christensen, K.T., Claudin, P., 2023. Field Evidence for the Initiation of Isolated Aeolian Sand Patches. *Geophys. Res. Lett.* 50(4), e2022GL101553. <https://doi.org/10.1029/2022GL101553>.
- Dong, Z., Wang, H., Liu, X., Wang, X., 2004. A wind tunnel investigation of the influences of fetch length on the flux profile of a sand dune blowing over a gravel surface. *Earth Surf. Proc. Land.* 29, 1613–1626. <https://doi.org/10.1002/esp.1116>.
- Dong, Z., Lv, P., Zhang, Z., Qian, G., Luo, W., 2012. Aeolian transport in the field: A comparison of the effects of different surface treatments. *J. Geophys. Res.* 117, D09210. <https://doi.org/10.1029/2012JD017538>.
- Durán Vinent, O., Moore, L.J., 2013. Vegetation controls on the maximum size of coastal dunes. *PNAS* 110, 17217–17222. <https://doi.org/10.1073/pnas.1307580110>.
- Durán Vinent, O., Moore, L.J., 2015. Barrier island bistability induced by biophysical interactions. *Nat. Clim. Chang.* 5, 158–162. <https://doi.org/10.1038/nclimate2474>.
- Gabriel, M.N., 2016. Gulf Islands to remove asphalt chunks, clean park. Retrieved from, Pensacola News Journal <https://www.pnj.com/story/news/2016/08/08/gulf-islands-remove-asphalt-chunks-and-clean-park/88268914/>.
- Gabriel, M.N., 2017. Fort Pickens asphalt removal project complete, more to come. Retrieved from, Pensacola News Journal <https://www.pnj.com/story/news/local/pensacola/beaches/2017/03/08/gulf-islands-national-seashore-asphalt-removal-bp-oil-spill/98876764/>.
- Gabriel, M.N., 2018. Is Gulf Islands National Seashore's asphalt removal project an exercise in futility? Pensacola News Journal. Retrieved from www.pnj.com/story/news/local/pensacola/beaches/2018/12/20/national-park-service-moves-ahead-11-million-asphalt-removal-project/2336325002/.
- Gillette, D.A., Stockton, P.H., 1989. The effect of nonerodible particles on wind erosion of erodible surfaces. *Journal of Geophysical Research: Atmosphere* 94, 12885–12893. <https://doi.org/10.1029/JD094iD10p12885>.
- Gillies, J.A., Lancaster, N., 2013. Large roughness element effects on sand transport, Oceano Dunes, California. *Earth Surface Processes and Landforms* 38 (8), 785–792. <https://doi.org/10.1002/esp.3317>.
- Gillies, J.A., Nickling, W.G., King, J., 2006. Aeolian sediment transport through large patches of roughness in the atmospheric inertial sublayer. *J. Geophys. Res.* Earth 2003–2012, 111. <https://doi.org/10.1029/2005JF000434>.
- Greeley, R., Iversen, J.D., 1985. *Wind as a Geological Process: On Earth, Mars, Venus, and Titan*. Cambridge University Press.
- Harrell, F.E., 2015. *Regression Modeling Strategies: With Applications to Linear Models, Logistic and Ordinal Regression, and Survival Analysis*. Springer.
- Hoonhout, B.M., De Vries, S., 2016. A process-based model for aeolian sediment transport and spatiotemporal varying sediment availability. *J. Geophys. Res.* Earth 121, 1555–1575. <https://doi.org/10.1002/2015JF003692>.
- Houser, C., 2009. Synchronization of transport and supply in beach-dune interaction. *Prog. Phys. Geogr.* 33, 733–746. <https://doi.org/10.1177/0309133309350120>.
- Houser, C., Barrett, G., 2009. Bed elevation changes in the upper-swash zone. *Journal of Coastal Research Special Issue No. 56*, 64–68. <http://www.jstor.org/stable/25737538>.
- Houser, C., Hapke, C., Hamilton, S., 2008. Controls on coastal dune morphology, shoreline erosion and barrier island response to extreme storms. *Geomorphology* 100, 223–240. <https://doi.org/10.1016/j.geomorph.2007.12.007>.
- Houser, C., Wernette, P., Rentschler, E., Jones, H., Hammond, B., Trimble, S., 2015. Post-storm beach and dune recovery: Implications for barrier island resilience. *Geomorphology* 234, 54–63. <https://doi.org/10.1016/j.geomorph.2014.12.044>.
- Iversen, J.D., Rasmussen, K.R., 1999. The effect of wind speed and bed slope on sand transport. *Sedimentology* 46, 723–731. <https://doi.org/10.1046/j.1365-3091.1999.00245.x>.
- Jackson, C.A., Schmutz, P.P., Harwell, M.C., Littles, C.J., 2020. The Ecosystem Service of Property Protection and Exposure to Environmental Stressors in the Gulf of Mexico. *Aeolian Res.* 184, 105017. <https://doi.org/10.1016/j.ocecoaman.2019.105017>.
- Lancaster, N., Baas, A., 1998. Influence of vegetation cover on sand transport by wind: Field studies at Owens Lake, California. *Earth Surf. Proc. Land.* 23, 69–82. [https://doi.org/10.1002/\(SICI\)1096-9837\(199801\)23:1<69::AID-ESP826>3.0.CO;2-G](https://doi.org/10.1002/(SICI)1096-9837(199801)23:1<69::AID-ESP826>3.0.CO;2-G).
- McKenna Neuman, C., 1998. Particle transport and adjustments of the boundary layer over rough surfaces with an unrestricted, upwind supply of sediment. *Geomorphology* 25, 1–17. [https://doi.org/10.1016/S0169-555X\(98\)00036-1](https://doi.org/10.1016/S0169-555X(98)00036-1).
- McKenna Neuman, C., Nickling, W.G., 1995. Aeolian sediment flux decay: Non-linear behaviour on developing deflation lag surfaces. *Earth Surf. Proc. Land.* 20, 423–435. <https://doi.org/10.1002/esp.3290200504>.
- McKenna Neuman, C., Bédard, O., 2017. A wind tunnel investigation of particle segregation, ripple formation and armouring within sand beds of systematically varied texture. *Earth Surf. Process. Landforms* 42, 749–762. <https://doi.org/10.1002/esp.4019>.
- McKenna Neuman, C., Li, B., Nash, D., 2012. Micro-topographic analysis of shell pavements formed by aeolian transport in a wind tunnel simulation. *Journal of Geophysical Research* 117. <https://doi.org/10.1029/2012JF002381>.
- McKenna Neuman, C., Sanderson, R.S., Sutton, S., 2013. Vortex shedding and morphodynamic response of bed surfaces containing non-erodible roughness elements. *Geomorphology* 198, 45–56. <https://doi.org/10.1016/j.geomorph.2013.05.011>.
- Mikami, M., Yamada, Y., Ishizuka, M., Ishimaru, T., Gao, W., Zeng, F., 2005. Measurement of saltation process over gobi and sand dunes in the Taklimakan desert, China, with newly developed sand particle counter. *J. Geophys. Res.* 110 (D18), D18S02.
- Miller, D.L., Thetford, M., Yager, L., 2001. Evaluation of sand fence and vegetation for dune building following overwash by Hurricane Opal on Santa Rosa Island, Florida. *J. Coast. Res.* 17, 936–948. <https://www.jstor.org/stable/4300253>.
- Nickling, W.G., McKenna Neuman, C., 1995. Development of deflation lag surfaces. *Sedimentology* 42, 403–414. <https://doi.org/10.1111/j.1365-3091.1995.tb00381.x>.
- Nield, J.M., 2011. Surface moisture-induced feedback in aeolian environments. *Geology* 39, 915–918. <https://doi.org/10.1130/G32151.1>.
- Owen, P.R., 1964. Saltation of uniform grains in air. *J. Fluid Mech.* 20, 225–242. <https://doi.org/10.1017/S0022112064001173>.
- R Core Team, 2024. *R: A Language and Environment for Statistical Computing*. R Foundation for Statistical Computing, Vienna, Austria <https://www.R-project.org>.
- Raupach, M.R., Gillette, D.A., Leys, J.F., 1993. The effect of roughness elements on wind erosion threshold. *J. Geophys. Res.* 98, 3023–3029. <https://doi.org/10.1029/92JD01922>.
- Rotnicka, J., 2013. Aeolian vertical mass flux profiles above dry and moist sandy beach surfaces. *Geomorphology* 187, 27–37. <https://doi.org/10.1016/j.geomorph.2012.12.032>.
- Rucker, J.B., Snowden, J.O., 1989. Relict Progradational Beach Ridge complex on Cat Island in Mississippi Sound. *AAPG Bulletin* 39.
- Schlichting, H., 1936. Experimentelle Untersuchungen zum Rauheitsproblem. *Arch. Appl. Mech.* 7, 1–34.
- Schmutz, P., Briggs, T., Tereszkiewicz, P., 2019. The utility of an omni-directional photoelectronic sensor device to measure meso-scale variability in aeolian sediment transport activity. *Aeolian Res.* 36, 61–67. <https://doi.org/10.1016/j.aeolia.2018.11.003>.
- Schwarz, G., 1978. Estimating the dimension of a model. *Ann. Stat.* 6. <https://doi.org/10.1214/aos/1176344136>.
- Sherman, D.J., Li, B., 2012. Predicting aeolian sand transport rates: A reevaluation of models. *Aeolian Res.* 3, 371–378. <https://doi.org/10.1016/j.aeolia.2011.06.002>.
- Sherman, D.J., Li, B., Ellis, J.T., Farrell, E.J., Maia, L.P., Granja, H., 2012. Recalibrating aeolian sand transport models. *Earth Surf. Proc. Land.* 38, 169–178. <https://doi.org/10.1002/esp.3310>.
- Sigren, J.M., Figlus, J., Highfield, W., Feagin, R.A., Armitage, A.R., 2018. The effects of coastal dune volume and vegetation on storm-induced property damage: Analysis from Hurricane Ike. *Journal of Coastal Research* 34 (1), 164–173. <https://doi.org/10.2112/JCOASTRES-D-16-00169.1>.
- Silva, R., Martinez, M.L., Oderiz, I., Mendoza, E., Feagin, R.A., 2016. Response of vegetated dune-beach systems to storm conditions. *Coast. Eng.* 109, 53–62. <https://doi.org/10.1016/j.coastaleng.2015.12.0070>.
- StataCorp., 2020. *Stata Statistical Software: Release 16.1*. StataCorp LLC., College Station, TX.
- Stone, G.W., Stapor, F.W., 1996. A nearshore sediment transport model for the northeast Gulf of Mexico Coast, U.S.A. *J. Coast. Res.* 12 (3), 786–792. <https://www.jstor.org/stable/4298524>.
- Stone, G.W., Stapor, F.W., May, J.P., Morgan, J.P., 1992. Multiple sediment sources and a cellular, non-integrated, longshore drift system: Northwest Florida and southeast Alabama coast, USA. *Mar. Geol.* 105, 141–154. [https://doi.org/10.1016/0025-3227\(92\)90186-L](https://doi.org/10.1016/0025-3227(92)90186-L).
- Sutton, S.L.F., McKenna Neuman, C., 2008. Variation in bed level shear stress on surfaces sheltered by nonerodible roughness elements. *J. Geophys. Res.* 113. <https://doi.org/10.1029/2007JF000967>.
- Swann, C., Lee, D., Trimble, S., Key, C., 2021. Aeolian sand transport over a wet, sandy beach. *Aeolian Res.* 51, 100712. <https://doi.org/10.1016/j.aeolia.2021.100712>.
- Tan, L., 2016. Aeolian sediment transport over gobi: Field studies atop the Mogao Grottoes, China. *Aeolian Res.* 21, 53–60. <https://doi.org/10.1016/j.aeolia.2016.03.002>.
- Tan, L., Zhang, W., Qu, J., Zhang, K., An, Z., Wang, X., 2013. Aeolian sand transport over gobi with different gravel coverages under limited sand supply: A mobile wind tunnel investigation. *Aeolian Res.* 11, 67–74. <https://doi.org/10.1016/j.aeolia.2013.10.003>.
- Udo, K., Kuriyama, Y., Jackson, D.W.T., 2008. Observations of wind-blown sand under various meteorological conditions at a beach. *J. Geophys. Res.* Earth 113 (F4).

- Valance, A., Rasmussen, K.R.m., Ould El Moctar, A., Dupont, P., 2015. The physics of Aeolian sand transport. *C. r. Phys.* 16 (1), 105–117.
- van der Wal, D., 1998. Effects of fetch and surface texture on aeolian sand transport on two nourished beaches. *J. Arid Environ.* 39 (3), 533–547. <https://doi.org/10.1006/jare.1997.0364>.
- Walker, I.J., Davidson-Arnott, R.G.D., Bauer, B.O., Hesp, P.A., Delgado-Fernandez, I., Ollerhead, J., Smyth, T.A.G., 2017. Scale-dependent perspectives on the geomorphology and evolution of beach-dune systems. *Earth Sci. Rev.* 171, 220–253. <https://doi.org/10.1016/j.earscirev.2017.04.011>.
- Wiggs, G.F.S., Atherton, R.J., Baird, A.J., 2004. Thresholds of aeolian sand transport: Establishing suitable values. *Sedimentology* 51, 95–108. <https://doi.org/10.1046/j.1365-3091.2003.00613.x>.